
Detection Rate of ^{18}F -Choline PET/CT and ^{68}Ga -PSMA-HBED-CC PET/CT for Prostate Cancer Lymph Node Metastases with Direct Link from PET to Histopathology: Dependence on the Size of Tumor Deposits in Lymph Nodes

Cordula A. Jilg¹, Vanessa Drendel², H. Christian Rischke^{3,4}, Teresa I. Beck⁴, Kathrin Reichel¹, Malte Krönig¹, Ulrich Wetterauer¹, Wolfgang Schultze-Seemann¹, Philipp T. Meyer^{4,5}, and Werner Vach^{6,7}

¹Department of Urology, Medical Center—University of Freiburg, Faculty of Medicine, University of Freiburg, Freiburg, Germany; ²Institute for Pathology, Faculty of Medicine, University of Freiburg, Freiburg, Germany; ³Department of Radiation Oncology, Medical Center—University of Freiburg, Faculty of Medicine, University of Freiburg, Freiburg, Germany; ⁴Department of Nuclear Medicine, Medical Center—University of Freiburg, Faculty of Medicine, University of Freiburg, Freiburg, Germany; ⁵German Cancer Consortium (DKTK), Partner Site Freiburg, Germany; ⁶Department of Orthopedics and Traumatology, University Hospital Basel, Switzerland; and ⁷Institute for Medical Biometry and Statistics, Faculty of Medicine & Medical Center, University of Freiburg, Freiburg, Germany

Accurate detection of prostate cancer lymph node metastases (LNM) through PET/CT before lymphadenectomy is crucial for successful therapy. PET/CT with choline derivatives used to be the standard tool for imaging metastases, whereas ^{68}Ga -PSMA (prostate-specific membrane antigen) PET/CT was introduced recently. Both PET techniques were investigated with respect to what extent the detection rate of LNM depends on the size of tumor deposits (TDs) within LNM. **Methods:** Documenting the switch from the use of ^{18}F -choline to ^{68}Ga -PSMA in 2014, we used 2 patient cohorts undergoing a template lymphadenectomy because of a PET/CT indicating LNM. Forty-four and 40 patients underwent PET/CT with ^{18}F -choline or ^{68}Ga -PSMA ligand, respectively. In total, 226 LNM (125 ^{18}F -choline, 101 ^{68}Ga -PSMA) originated from 73 salvage lymphadenectomies at biochemical recurrence and from 11 primary lymphadenectomies at radical prostatectomy. LNM eligible for direct correlation of PET/CT to histopathology were identified from lymphadenectomies conducted in small anatomic subregions, with 1 LNM (condition 1) or 1–2 LNM (condition 2). Longitudinal and short diameters of TD within LNM were determined by histopathology, allowing linking of the size of TD in LNM to the detection threshold of PET/CT. Diameters associated with a detection rate of 50% and 90% ($d_{50\%}$, $d_{90\%}$) were calculated on the basis of logistic growth curve models fitted. **Results:** Gleason score, number of removed LNs, and subregions for lymphadenectomy per patient did not differ significantly between the ^{18}F -choline and ^{68}Ga -PSMA groups. The median prostate-specific antigen level at imaging and number of LNM per patient were significantly higher in the ^{18}F -choline group (3.4 ng/mL, $n = 34$) than in the ^{68}Ga -PSMA group (2.2 ng/mL, $n = 28$; both $P < 0.05$). Longitudinal and short diameters of TD in LNM to reach $d_{90\%}$ were 11.2 and 7.4 mm, respectively, for ^{18}F -choline PET/CT and 6.3 and 4.9 mm, respectively, for ^{68}Ga -PSMA PET/CT. Corresponding diameters to reach $d_{50\%}$ were 5.5 and 3.3 mm, respectively, for ^{18}F -choline PET/CT and 3.7 and 2.3 mm, respectively, for ^{68}Ga -PSMA PET/CT. Detection rates were significantly higher under ^{68}Ga -PSMA ($P = 0.005$ and 0.04 for longitudinal and

short diameter). **Conclusion:** ^{68}Ga -PSMA PET/CT is superior to ^{18}F -choline PET/CT in the detection of LNM. Whether those results will lead to an improved patient outcome after ^{68}Ga -PSMA PET-guided therapy needs to be investigated by further studies.

Key Words: prostate cancer; lymph node metastases; PSMA-PET/CT; choline-PET/CT; detection rate

J Nucl Med 2019; 60:971–977

DOI: 10.2967/jnumed.118.220541

A precise detection of lymph node (LN) metastases (LNM) in prostate cancer (PCa) is fundamental at primary diagnosis and at the stage of biochemical recurrence (BR) with PCa relapse (mainly due to LNM) to plan and conduct the most adequate therapy (1–3). Surgical resection of LNM through pelvic lymphadenectomy associated with radical prostatectomy (RP) in the case of primary therapy or associated with salvage lymph node dissection (salvage lymphadenectomy) in the case of BR are approaches offered to patients with suspected LNM. Those therapies might be able to reduce the tumor burden significantly, delay clinical progression, and avoid early systemic treatment such as hormone deprivation therapy (ADT) or chemotherapy (1,2,4).

As conventional imaging modalities such as CT and MRI exhibit a limited sensitivity for LNM detection (5), PET/CT with choline analogs such as ^{18}F -fluoroethyl-choline or ^{11}C -choline was the standard tool for imaging PCa lesions for many years. PET/CT imaging of the expression of the prostate-specific membrane antigen (PSMA) was introduced only recently (3,5–9). Targeting PSMA on the surface of PCa cells allows for powerful imaging of PCa lesions (8,10,11). The superiority of ^{68}Ga -PSMA PET/CT compared with ^{18}F -choline PET/CT with respect to general diagnostic accuracy has been analyzed by different groups (3,12,13). These studies did not, however, stratify the results by the size of the tumor deposits (TDs) in LNMs (3).

In this present study, we extend these investigations by analyzing to what extent the detection of LNMs depends on the size of the TD in LNM from lymphadenectomy after ^{18}F -choline PET/CT or ^{68}Ga -PSMA PET/CT. Such an investigation requires LNMs for

For correspondence or reprints contact: Cordula A. Jilg, Department of Urology, University of Freiburg, Hugstetterstraße 55, 79106 Freiburg, Germany. E-mail: cordula.jilg@uniklinik-freiburg.de
Published online Jan. 25, 2019.
COPYRIGHT © 2019 by the Society of Nuclear Medicine and Molecular Imaging.

which we can establish a direct correlation from the PET/CT results to histopathology, as the latter evaluates subregions, not single LNMs. A direct correlation is possible, if there is only 1 LNM (verified by histopathology) in 1 subregion rated by PET/CT. This allowed us to compare the detection rates for TD in LNMs of a given size between ^{18}F -choline PET/CT and ^{68}Ga -PSMA PET/CT. Describing the conversion from ^{18}F -choline (2007–2014) to ^{68}Ga -PSMA in 2014, we used 2 available patient cohorts from our clinic undergoing a template lymphadenectomy because of a PET/CT indicating LNM (11,14). From both cohorts, subregions eligible for conditions 1 and 2 were included in this study. Data were collected from 73 patients at the stage of BR undergoing a salvage lymphadenectomy and from 11 men at the stage of primary therapy (RP with extended lymphadenectomy). The detection rate of PET/CT on the size of TD in LNM was investigated in 125 (^{18}F -choline) and 101 LNMs (^{68}Ga -PSMA). Diameters associated with a detection rate of 50% and 90% ($d_{50\%}$, $d_{90\%}$) were calculated on the basis of logistic growth curve models fitted.

MATERIALS AND METHODS

Study Goal and Design

The aim of this retrospective study was to analyze the dependence of the LNM detection rate of ^{18}F -choline and ^{68}Ga -PSMA PET/CT on the size of the TD in LNM from salvage lymphadenectomy and primary lymphadenectomy. Such an investigation requires LNMs for which we can establish a direct correlation from the PET/CT results to histopathology, as the latter evaluates subregions, not single LNMs. A direct correlation is possible, if there is only 1 LNM (verified by histopathology) in 1 subregion. If there are 2 LNMs in 1 subregion and only 1 is detected, we do not know exactly which one was detected, but mathematic modeling still allows us to establish a link. In our study, we therefore considered only subregions with 1 or 2 LNMs, allowing us to compare the detection rates for TD in LNMs of a given size between ^{18}F -choline PET/CT and ^{68}Ga -PSMA PET/CT. Because the analysis of subregions with 1 LNM is easier than the analysis with

2 LNMs, we present results both for subregions with only 1 LNM (condition 1) and for subregions with 1 or 2 LNMs (condition 2) (Supplemental Fig. 1; supplemental materials are available at <http://jnm.snmjournals.org>).

Source of Patients

We used 1 patient cohort undergoing a template lymphadenectomy because of a PET/CT indicating LNM at our clinic and (published previously (11,14)) supplemented by patients with lymphadenectomy at RP at our center. Because of a shift from ^{18}F -choline to ^{68}Ga -PSMA as the tracer for PET/CT in 2014, this cohort can be divided into 2 corresponding groups. In each group, those patients with at least 1 subregion satisfying condition 1 or condition 2 were selected: 44 individuals in the ^{18}F -choline group originated from the patient cohort published in 2014 by our group ($n = 72$) (14). Twenty-nine of 40 individuals from the ^{68}Ga -PSMA group originated from the patient cohort published in 2017 by our group ($n = 30$) (11); the remaining 11 patients underwent an extensive template lymphadenectomy at RP between November 2014 and December 2015 (Table 1; Fig. 1). The institutional review board approved this study (No. 562/15), and all subjects signed a written informed consent form.

PET Tracer

^{18}F -choline PET/CT was the available tracer for imaging PCa patients at BR from 2007 to 2014. In 2014, ^{68}Ga -PSMA PET/CT was introduced at our center and replaced ^{18}F -choline PET/CT. We therefore observed the shift from ^{18}F -choline to ^{68}Ga -PSMA with respect to LNM detection.

LNMs Available

Overall, 84 patients provided subregions with 1 single LNM (condition 1) and 1 or 2 LNMs (condition 2) verified by histopathology (Fig. 1; Table 1; Supplemental Fig. 1). For condition 1, we included 52 detected and 21 undetected single LNMs in the ^{18}F -choline PET/CT group and 55 detected and 18 undetected LNMs in the ^{68}Ga -PSMA PET/CT group; for condition 2, we included 74 detected and 51 undetected LNMs in the ^{18}F -choline PET/CT group and 72 detected and 29 undetected LNMs in the ^{68}Ga -PSMA PET/CT group (Table 1).

TABLE 1
Clinical Characteristics from 84 PCa Patients Undergoing Lymphadenectomy

Variable	^{18}F -choline PET/CT ($n = 44$ patients)	^{68}Ga -PSMA PET/CT ($n = 40$ patients)	<i>P</i> (Mann–Whitney test)
Lymphadenectomy (n)			—
Primary	0	11	
Salvage	44	29	
Mean age \pm SD at surgery (y)	65.6 \pm 5.8 (65.8)	66.1 \pm 6.6 (67.3)	0.720
Mean Gleason score \pm SD	7.8 \pm 0.84 (8)	7.6 \pm 0.9 (7)	0.230
Mean PSA at surgery (ng/mL) \pm SD	9 \pm 14.0 (3.4)	4.8 \pm 7.2 (2)	0.038
Mean time from PET/CT to surgery (mo) \pm SD	2.1 \pm 1.7 (1.8)	2.6 \pm 1.9 (2.1)	0.1077
LN/LNM removed overall (n)	1,542/485	1,188/183	—
Mean LNs removed per patient \pm SD (n)	34.3 \pm 19.9 (34)	30.5 \pm 15.3 (28)	0.373
Mean LNM removed per patient \pm SD (n)	10.8 \pm 13.3 (4)	4.7 \pm 6.7 (3)	0.0048
Mean subregions for lymphadenectomy per patient \pm SD (n)	7.3 \pm 2.9 (8)	7.7 \pm 2.9 (8)	0.443
Mean number of LNs removed per subregion \pm SD (n)	4.6 \pm 1.8 (4.2)	4.1 \pm 1.8 (3.7)	0.229
Mean LNM density (%) (LNM \times 100/LNs removed) \pm SD	32.2 \pm 28.5 (25)	17.1 \pm 19.7 (10.7)	0.0063

Data in parentheses are median.
PSA = prostate-specific antigen.

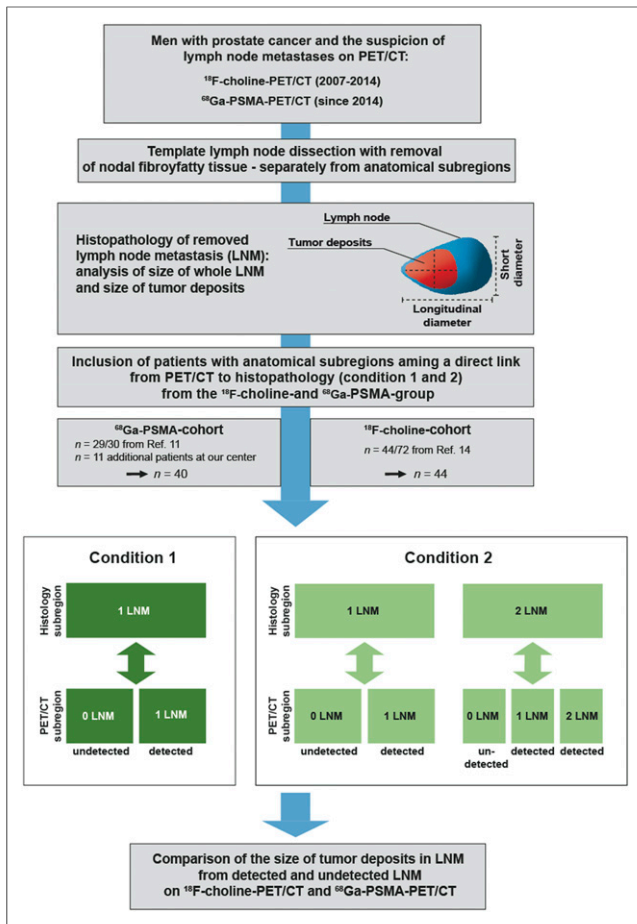


FIGURE 1. Workflow with surgery, tissue sample processing, and identification of eligible subregions in men with suspected nodal metastatic PCa undergoing a template lymphadenectomy after PET/CT. Tissue specimens from small anatomic subregions were removed separately at surgery. At histopathology, the size of TDs was determined. Aiming at a direct link from PET/CT to histopathology, subregions fulfilling the requirement for conditions 1 and 2 were selected from ^{18}F -choline and the ^{68}Ga -PSMA PET/CT groups. Finally, size of TDs in detected and undetected LNMs was evaluated for estimation of detection thresholds.

^{18}F -Choline-PET/CT and ^{68}Ga -PSMA-HBED-CC PET/CT Imaging Analysis

The ^{18}F -choline PET/CT and ^{68}Ga -PSMA PET/CT were conducted as previously described by Jilg et al. (11,14). PET/CT was performed after intravenous injection of a mean activity \pm SD of 245 ± 40.5 MBq of ^{18}F -fluoroethylcholine and 189.6 ± 32.6 MBq of ^{68}Ga -PSMA (Glu-NH-CO-NH-Lys-(Ahx)-[^{68}Ga (HBED-CC)]) with image acquisition starting 45–60 min after injection. Transverse PET/CT slices, 3 mm in thickness, were generated. CT data were used to correct for photon attenuation. A ^{18}F -choline- or a PSMA-positive lesion was defined as a focal tracer accumulation greater than normal or physiologic local background activity. Two experienced nuclear medicine physicians evaluated all the PET/CT studies in consensus by side-by-side review of the coregistered PET and CT datasets using predefined PET window settings (inverted gray scale; SUV range, 0–5 g/mL) (PAXCS and IMPAX workstation [AGFA Health Care]). The 2 PET/CT readers were masked to the data from histopathology.

Lymphadenectomy

Salvage Lymphadenectomy. Patients at the stage of BR (PSA > 0.2 ng/mL in 2 consecutive measurements) after primary therapy and the suspicion

of LNM (without detectable bone or visceral metastases) in an ^{18}F -choline PET/CT ($n = 44$) or ^{68}Ga -PSMA PET/CT ($n = 29$) underwent a salvage lymphadenectomy on a compassionate-use basis. Depending on the presence of PET-positive lesions (pelvic, retroperitoneal, or both), a bilateral template pelvic lymphadenectomy (subregions: common iliac vessels, external iliac vessels, obturator vessels, internal iliac vessels, presacral region), a retroperitoneal lymphadenectomy (subregions: aortic bifurcation, aortal, caval, interaortocaval), or combined pelvic and retroperitoneal lymphadenectomy was conducted.

Primary Lymphadenectomy. Eleven patients underwent a primary extended lymphadenectomy at RP after a ^{68}Ga -PSMA PET/CT with the suspicion of LNMs. Because of the presence of PET-positive pelvic regions, a bilateral template pelvic lymphadenectomy (subregions: common iliac vessels, external iliac vessels, obturator vessels, internal iliac vessels, presacral region) was conducted.

Generally, whenever intraoperative circumstances permitted, we adhered to the templates at salvage lymphadenectomy or primary lymphadenectomy and removed the nodal-fibro-fatty tissue. During lymphadenectomy, LN portions from each subregion were collected separately.

Histopathology

All resected LNMs were formalin-fixed and paraffin-embedded, followed by histopathologic evaluation by 1 pathologist on hematoxylin and eosin-stained tissue slides. The pathologist was not aware of the PET findings nor was he informed about the clinical results provided by the surgeon. The longitudinal diameter and short diameter of each whole LNM and TDs were measured under the microscope, in millimeters,

TABLE 2
Number of LNMs Included for Conditions 1 and 2 from ^{18}F -Choline and ^{68}Ga -PSMA PET/CT Groups

Condition	^{18}F -choline-PET/CT ($n = 44$ patients)	^{68}Ga -PSMA-PET/CT ($n = 40$ patients)	Total
1			
Individuals (n)	38	38	76
Subregions (n)	73	73	146
LNM overall (n)	73	73	146
True-positive LNM	52	55	107
False-negative LNM	21	18	29
2			
Individuals (n)	44	40	84
Additional subregions (n)	26	14	40
0 LNM at PET, 2 LNMs at histology	10	3	13
1 LNM at PET, 2 LNMs at histology	10	5	15
2 LNM at PET, 2 LNMs at histology	6	6	12
LNM overall (n)	125	101	226
True-positive LNM	74	72	146
False-negative LNM	51	29	80

using a ruler. The short diameter represents the maximum diameter we could observe when looking orthogonal in the direction of the longitudinal diameter. Area and volume of the TD in LNM were determined assuming an ellipsoid shape and hence the following formulas were used:

$$\text{Area [mm}^2\text{]} = (\pi \times \text{longitudinal diameter} \times \text{short diameter}) / 4.$$

$$\text{Volume [mm}^3\text{]} = 4/3 \times (\pi \times \text{longitudinal diameter} \times \text{short diameter} \times \text{short diameter}) / 8.$$

Statistics

The outcome of interest was the detection of an LNM, that is, a true-positive result of PET/CT. In a first step, we divided the LNMs identified under condition 1 according to their longitudinal and short diameter in intervals of 1 mm in length and considered the empiric detection rate in each interval, that is, the proportion of LNMs detected by PET/CT. We fitted logistic growth curve models, describing the probability (on the logit scale) of detecting an LNM as a linear function $\alpha + \beta d$ of the diameter d . From these models, we estimated the diameters $d_{50\%}$ and $d_{90\%}$ associated with a detection rate of 90% and 50%, respectively. Fitting such models is also possible under condition 2, allowing the relation of 2 diameters to the observed PET/CT results; details are given in the Supplemental Appendix. The statistical significance of the overall trend toward smaller or greater detection rates in 1 group was assessed by fitting a joint growth curve model so as to allow only a shift between the 2 curves. To judge the clinical relevance of the estimated diameters associated with a certain detection rate, we also determined the relative frequency of LNMs with diameters exceeding the estimated ones. These numbers

estimate the actually observed fractions of LNMs with detection probabilities above 50% or 90% in our clinical sample, respectively. Statistical computations are based on Stata 14.2 (StataCorp [https://www.stata.com/]) and Prism7 software (GraphPad).

RESULTS

Clinical Parameters and Results from Lymphadenectomy

Age at surgery, Gleason score, time from PET/CT to surgery, number of removed LN and LNMs, subregions for lymphadenectomy per patient, and number of removed LN per subregion did not differ between the individuals who underwent ^{18}F -choline PET/CT or ^{68}Ga -PSMA PET/CT. In contrast, men from the ^{18}F -choline PET/CT cohort exhibited a higher PSA level and a higher number of LNMs than did those in the ^{68}Ga -PSMA PET/CT group (Table 1). Figure 1 shows the workflow concerning patient selection, surgery, histopathologic workup, and our approach for the evaluation of the detection rates (conditions 1 and 2). Four representative examples (PET with corresponding CT) of LNM with direct link from PET to histopathology on a ^{18}F -choline PET/CT or ^{68}Ga -PSMA PET/CT are shown in Supplemental Figures 2A and 2B. Clinical parameters and data from lymphadenectomy are listed in Table 1. Information about the number of LNMs for conditions 1 and 2 for both tracer groups are shown in Table 2.

Characteristics of LNMs

The distribution of the longitudinal diameter and short diameter and area and volume of TDs in detected or overlooked LNMs under condition 1 (overall $n = 146$ LNMs) by ^{18}F -choline PET/CT ($n = 73$ subregions, LNM) or ^{68}Ga -PSMA PET/CT ($n = 73$ subregions, LNM) are described in Supplemental Table 1.

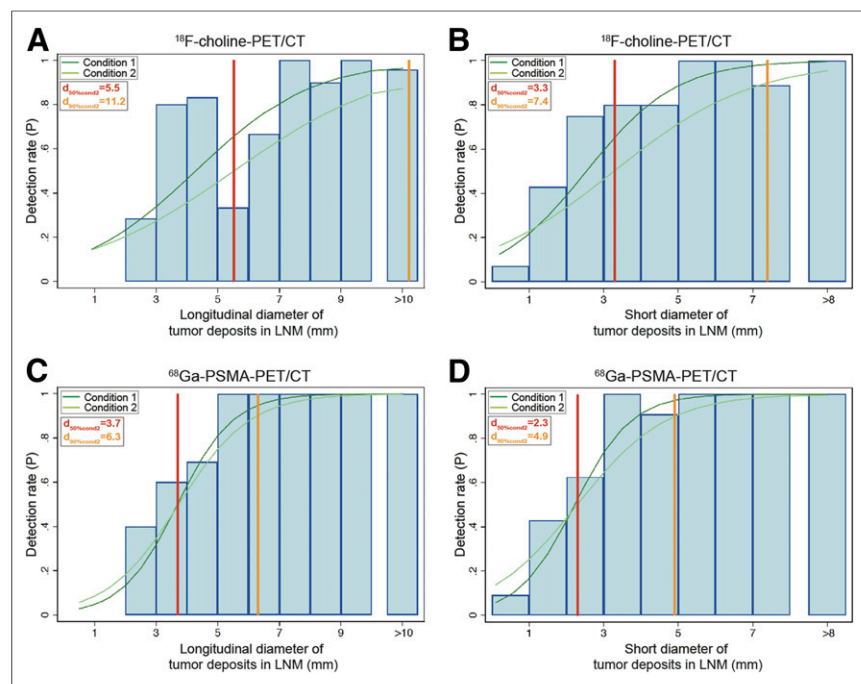


FIGURE 2. (A–D) Empiric detection rates from ^{18}F -choline PET/CT and the ^{68}Ga -PSMA PET/CT groups for conditions 1 and 2 in dependence on diameter of TD (divided into intervals of 1 mm in length). Dark green line (condition 1) and light green line (condition 2) represent the fitted logistic growth curve model and red line the estimated diameters $d_{90\%}$ and $d_{50\%}$, respectively. Longitudinal diameters (A and C) above 10 mm and short diameters (B and D) above 8 mm are shown as 1 group.

Detection Rates

The relation of detection rates for ^{18}F -choline PET/CT or ^{68}Ga -PSMA PET/CT to diameters is visualized in Figures 2 and 3, including visualizations of the fitted growth curves and the determination of the thresholds $d_{50\%}$ and $d_{90\%}$. Estimates of the necessary size (longitudinal diameter and short diameter), area and volume to achieve a $d_{50\%}$, and $d_{90\%}$ detection rate of ^{18}F -choline PET/CT or ^{68}Ga -PSMA PET/CT are shown in Table 3.

$d_{50\%}$ and $d_{90\%}$ values tend to be smaller with ^{68}Ga -PSMA PET/CT than with ^{18}F -choline PET/CT. Overall, the difference in detection rates was significant under condition 2. For ^{18}F -choline PET/CT, the results for condition 2 suggest that a longitudinal diameter of 11.2 or 5.5 mm is sufficient to reach a detection probability of 90% or 50%, respectively (corresponding values for the short diameter are 7.4 and 3.3 mm). When ^{68}Ga -PSMA PET/CT is used, the results for condition 2 suggest that a longitudinal diameter of 6.3 or 3.7 mm is sufficient to reach a detection probability of 90% or 50%, respectively. The corresponding values for the short diameter are 4.9 and 2.3 mm.

Table 3 also suggests that we can reach with ^{68}Ga -PSMA PET/CT a detection probability of $\geq 90\%$ for about half of all LNMs

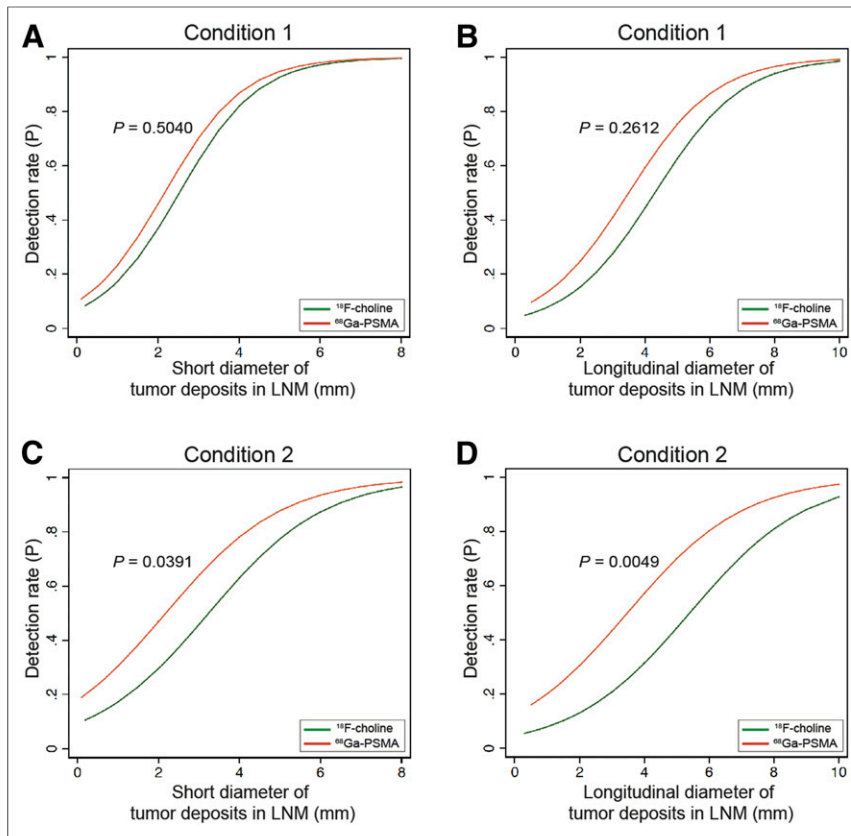


FIGURE 3. Empiric detection rate for condition 1 (A and B) and 2 (C and D) in dependence on diameter of TD. Fitted logistic growth curve models for ^{18}F -choline PET/CT and ^{68}Ga -PSMA PET/CT and P value for difference between the 2 curves are shown.

considered and a detection probability of $\geq 50\%$ for about three quarters. The respective figures for ^{18}F -choline PET/CT (19% and 57%, respectively) indicate a considerably worse performance.

DISCUSSION

Regarding only size of LN at CT or MRI, a large number of existing LNMs will be missed because of the presence of micrometastases (15). Consequently, the pooled sensitivity for CT and MRI was reported to be 42% and 39%, respectively, whereas the pooled specificity was 82% for both CT and MRI (5). PET/CT with ^{18}F -choline analogs such as ^{18}F -fluoroethylcholine or ^{11}C -choline provided respectable results for LN staging of PCa; estimates for sensitivity (38%–98%) and specificity (40%–100%), however, turned out to be fairly variable (7). The superiority of ^{68}Ga -PSMA PET/CT to PET/CT with ^{18}F -choline analogs for the detection of PCa lesions (e.g., LNM) with respect to overall accuracy has already been demonstrated by several studies (12,13,16). However, histopathologic data about the minimum tumor load (e.g., TDs in LNM) triggering a positive PET finding are scarce for both tracers (12,13,16).

By applying semiautomatic LN segmentation software, Giesel et al. assessed the LN volume and size of ^{68}Ga -PSMA PET-positive LNMs in 49 LNMs from 21 men with PCa relapse (17). They reported a mean short and longitudinal axis of ^{68}Ga -PSMA PET-positive LNMs of 5.8 and 9.5 mm. In line with our data, the detection limit was below the CT/MRI criteria of 8–10 mm (15). However, a histologic verification of ^{68}Ga -PSMA PET-positive LNMs and a consideration of the TD alone were not reported (17).

Measurements of TD in 34 LNMs (median, 13.6 mm) detected and 19 LNMs (median, 4.3 mm) undetected by PSMA PET/CT from 12 men after lymphadenectomy at RP by Budäus et al. (18) deviate markedly from our data and the data provided by Giesel et al. (17). In that report, the approach of anatomic correlation of PET and histopathology was not, however, reported in detail (18).

Unique features of our investigation are the approach of identification of LNM with a direct link from PET/CT to histopathology (conditions 1 and 2) and the considering of TDs in LNM for estimating the detection rates. A necessary short diameter of TD in LNM of 3.9 mm to reach a $d_{90\%}$ with ^{68}Ga -PSMA PET/CT (condition 1, Table 3) impressively underlines the fact that lesions of small size (i.e., well below the scanner spatial resolution of about 6–7 mm) can nevertheless be detected with high sensitivity if target expression is high. To corroborate our results from condition 1 analysis (1 LNM per subregion), we repeated this calculation with an increased sample size, also including subregions with 2 verified LNMs (condition 2). This yielded comparable results.

The performance of both tracers in detecting PCa lesions is correlated to the expression and metabolism of choline transports or the expression of PSMA in the membrane of PCa cells (19–21), for example. Choline transporters (e.g., CHT1s and CTL1) (19,20) are essentially involved when choline is rapidly cleared from the blood pool and incorporated into PCa cells (20); differences of their expression in relapsed and primary PCa are well described (22,23). For PSMA, it is known that about 8% of the primary high-risk PCa patients will not present with a tracer enhancement in a ^{68}Ga -PSMA PET/CT (24,25). With respect to the PSMA study population investigated in 2017 (11), we highlighted the correlation of SUV_{max} in LNM, the intensity of anti-PSMA immunohistochemistry, and the diameter of TD in the LNM (11): all the LNMs on hematoxylin and eosin staining were clearly positive for anti-PSMA, meaning that no LNM had been missed because of a lack of PSMA expression. For LNMs with a direct link from PET/CT to histopathology, a correlation of SUV_{max} with the area-weighted PSMA score was not significantly different ($r = 0.1536$ $P = 0.3136$; 95% confidence interval, -0.155 to 0.435). In contrast, a correlation of SUV_{max} with the maximum diameter of the TDs in the LNM was highly significant ($r = 0.6720$ $P < 0.0001$; 95% confidence interval, 0.464 – 0.809) (11).

As we investigated in our work PET-positive patients (PET-positive LNMs) exclusively, however, the heterogeneity mentioned above might be limited. Furthermore, differences of choline transporter and PSMA expression within 1 patient (e.g., between LNMs from 1 primary tumor) are not clearly investigated and probably more unlikely than between individuals. In summary, we suppose that the variation of choline transporter expression or PSMA expression might not be a significant bias in this analysis.

Our results regarding the histopathologic minimum tumor load in LNMs for detection of metastases through ^{18}F -choline or

TABLE 3

Estimated Diameters Associated with Detection Rates of d_{90%} and d_{50%}, Respectively, for Both Conditions, Stratified for ¹⁸F-Choline PET/CT and ⁶⁸Ga-PSMA PET/CT

Condition	¹⁸ F-choline PET/CT				⁶⁸ Ga-PSMA PET/CT			
	d _{90%}	Frequency of cases above d _{90%}	d _{50%}	Frequency of cases above d _{50%}	d _{90%}	Frequency of cases above d _{90%}	d _{50%}	Frequency of cases above d _{50%}
1								
Longitudinal diameter (mm)	8.5	42.4%	4.3	66.4%	5.7	49.5%	3.7	73.3%
Short diameter (mm)	5.2 m	38.4%	2.5	66.4%	3.9	54.5%	2.2	72.3%
Area (mm ²)	36.4	37.6%	11.7	61.6%	15.9	54.5%	7.8	70.3%
Volume (mm ³)	152.1	34.4%	35.6	56.8%	40.5	55.4%	16.1	67.3%
2								
Longitudinal diameter (mm)	11.2	19.2%	5.5	56.8%	6.3	47.5%	3.7	73.3%
Short diameter (mm)	7.4	23.2%	3.3	56.8%	4.9	46.5%	2.3	72.3%
Area (mm ²)	62.7	20.8%	18.8	52.8%	22.4	43.6%	8.5	67.3%
Volume (mm ³)	387.1	16.8%	66.0	47.2%	72.6	42.6%	19.1	66.3%

⁶⁸Ga-PSMA PET/CT are remarkable by themselves, regardless of the comparison of both tracers. Whether a lymphadenectomy after ⁶⁸Ga-PSMA PET/CT or ¹⁸F-choline PET/CT changes the fate of a patient with nodal metastases remains to be seen. Several more clinical parameters such as timing of surgery, tumor load, and the extent on lymphadenectomy will determine whether a patient will benefit from surgery or not.

Although we could demonstrate that when using PSMA PET/CT, in particular, detection rates can be remarkably high for diameters below the scanner resolution, we are still faced with the fact that small LNMs will be overlooked. After the attempt of removing all potential pelvic LNMs, a target lymphadenectomy in PET-positive regions only will not be universal as PET-negative subregions might harbor small LNMs remaining undetected. A systematic bilateral lymphadenectomy should therefore still be performed. Our data indicate that if available, a ⁶⁸Ga-PSMA PET/CT should be preferred to ¹⁸F-choline PET/CT to reveal LNMs. There are probably additional circumstances (tumor activity in LNM, PSMA-negativity) determining whether an LNM will be detected or not. Of course, it is therefore necessary to improve the detection rate of currently used tracers. Whether an improved detection rate, and thereby an assumed complete surgical resection, or target radiotherapy will lead to a significantly improved outcome in those metastasized patients is yet to be seen.

This study had limitations. Actually, patients with eligible sub-region for condition 1, 2 were included in this study, regardless of the character of the clinical data. We therefore had to register the clinical data (such as PSA level and number of LNMs) as they were present at the time of PET imaging with respect to surgery. The aim of Table 1, however, is to highlight that the clinical data from both groups were predominantly balanced.

The number of available LNMs in both cohorts was limited. This is a consequence of the need to identify LNMs for which a direct link to the PET/CT results could be established. Using only subregions with a single LNM is a clear and well-defined approach to establish this link. In the ⁶⁸Ga-PSMA PET/CT group in particular, however, only a few PET/CT-negative LNMs of this type could be found (reflecting already the superiority of PSMA in detecting small LNMs). We hence enlarged both groups by applying condition 2. This increase in sample size allowed us to demonstrate a significant

overall difference in detection rates between ¹⁸F-choline and ⁶⁸Ga-PSMA PET/CT.

LNM samples of the ¹⁸F-choline and the ⁶⁸Ga-PSMA PET/CT analyses originated from different patient populations. This limitation would be circumvented by performing a combined ¹⁸F-choline and ⁶⁸Ga-PSMA PET/CT in a prospective study cohort. However, given the expected limited additional clinical value of an ¹⁸F-choline PET/CT scan (when a ⁶⁸Ga-PSMA PET/CT is available) and the considerably higher radiation, financial, and logistic burden of a dual-tracer approach, we chose to analyze our well-defined earlier patients cohorts.

Because only patients with known BR relapse and the suspicion of LNM on ¹⁸F-choline or ⁶⁸Ga-PSMA PET/CT have been included in this study, our patient cohort is biased toward patients with tumor manifestations that show sufficient ¹⁸F-choline uptake and PSMA expression. This, however, is a general prerequisite for ¹⁸F-choline and ⁶⁸Ga-PSMA PET/CT that needs to be kept in mind.

CONCLUSION

In line with earlier studies demonstrating a higher diagnostic accuracy of ⁶⁸Ga-PSMA PET/CT than PET/CT with ¹⁸F-choline analogs for identification of LNMs, the present study suggests the detection limit of TDs is lower for ⁶⁸Ga-PSMA PET/CT. Whether this results in an improved outcome of patients undergoing ⁶⁸Ga-PSMA PET/CT-guided lymphadenectomy needs to be investigated further.

DISCLOSURE

No potential conflict of interest relevant to this article was reported.

REFERENCES

1. Cornford P, Bellmunt J, Bolla M, et al. EAU-ESTRO-SIOG guidelines on prostate cancer: part II—treatment of relapsing, metastatic, and castration-resistant prostate cancer. *Eur Urol*. 2017;71:630–642.
2. Mottet N, Bellmunt J, Bolla M, et al. EAU-ESTRO-SIOG guidelines on prostate cancer: part I—screening, diagnosis, and local treatment with curative Intent. *Eur Urol*. 2017;71:618–629.

3. Rauscher I, Maurer T, Beer AJ, et al. Value of ^{68}Ga -PSMA HBED-CC PET for the assessment of lymph node metastases in prostate cancer patients with biochemical recurrence: comparison with histopathology after salvage lymphadenectomy. *J Nucl Med*. 2016;57:1713–1719.
4. Abdollah F, Briganti A, Montorsi F, et al. Contemporary role of salvage lymphadenectomy in patients with recurrence following radical prostatectomy. *Eur Urol*. 2015;67:839–849.
5. Hövels AM, Heesakkers RA, Adang EM. The diagnostic accuracy of CT and MRI in the staging of pelvic lymph nodes in patients with prostate cancer: a meta-analysis. *Clin Radiol*. 2008;63:387–395.
6. Perera M, Papa N, Christidis D, et al. Sensitivity, specificity, and predictors of positive ^{68}Ga -prostate-specific membrane antigen positron emission tomography in advanced prostate cancer: a systematic review and meta-analysis. *Eur Urol*. 2016;70:926–937.
7. Picchio M, Briganti A, Fanti S, et al. The role of choline positron emission tomography/computed tomography in the management of patients with prostate-specific antigen progression after radical treatment of prostate cancer. *Eur Urol*. 2011;59:51–60.
8. Afshar-Oromieh A, Malcher A, Eder M, et al. PET imaging with a [^{68}Ga]gallium-labelled PSMA ligand for the diagnosis of prostate cancer: biodistribution in humans and first evaluation of tumour lesions. *Eur J Nucl Med Mol Imaging*. 2013;40:486–495.
9. Rahbar K, Weckesser M, Huss S, et al. Correlation of intraprostatic tumor extent with (6)(8)Ga-PSMA distribution in patients with prostate cancer. *J Nucl Med*. 2016;57:563–567.
10. Eder M, Neels O, Muller M, et al. Novel preclinical and radiopharmaceutical aspects of [^{68}Ga]Ga-PSMA-HBED-CC: a new PET tracer for imaging of prostate cancer. *Pharmaceuticals (Basel)*. 2014;7:779–796.
11. Jilg CA, Drendel V, Rischke HC, Becke TI, Vach W. Diagnostic accuracy of Ga-68-HBED-CC-PSMA-Ligand-PET/CT before salvage lymph node dissection for recurrent prostate cancer. *Theranostics*. 2017;7:1770–1780.
12. Afshar-Oromieh A, Zechmann CM, Malcher A, et al. Comparison of PET imaging with a ^{68}Ga -labelled PSMA ligand and ^{18}F -choline-based PET/CT for the diagnosis of recurrent prostate cancer. *Eur J Nucl Med Mol Imaging*. 2014;41:11–20.
13. Pfister D, Porres D, Heidenreich A, et al. Detection of recurrent prostate cancer lesions before salvage lymphadenectomy is more accurate with ^{68}Ga -PSMA-HBED-CC than with ^{18}F -Fluoroethylcholine PET/CT. *Eur J Nucl Med Mol Imaging*. 2016;43:1410–1417.
14. Jilg CA, Schultze-Seemann W, Drendel V, et al. Detection of lymph node metastasis in patients with nodal prostate cancer relapse using F/C-choline positron emission tomography/computerized tomography. *J Urol*. 2014;192:103–110.
15. Torabi M, Aquino SL, Harisinghani MG. Current concepts in lymph node imaging. *J Nucl Med*. 2004;45:1509–1518.
16. Morigi JJ, Stricker PD, van Leeuwen PJ, et al. Prospective comparison of ^{18}F -fluoromethylcholine versus ^{68}Ga -PSMA PET/CT in prostate cancer patients who have rising PSA after curative treatment and are being considered for targeted therapy. *J Nucl Med*. 2015;56:1185–1190.
17. Giesel FL, Fiedler H, Stefanova M, et al. PSMA PET/CT with Glu-urea-Lys-(Ahx)-[^{68}Ga (HBED-CC)] versus 3D CT volumetric lymph node assessment in recurrent prostate cancer. *Eur J Nucl Med Mol Imaging*. 2015;42:1794–1800.
18. Budäus L, Leyh-Bannurah SR, Salomon G, et al. Initial experience of ^{68}Ga -PSMA PET/CT imaging in high-risk prostate cancer patients prior to radical prostatectomy. *Eur Urol*. 2016;69:393–396.
19. Müller SA, Holzappel K, Seidl C, Treiber U, Krause BJ, Senekowitsch-Schmidtko R. Characterization of choline uptake in prostate cancer cells following bicalutamide and docetaxel treatment. *Eur J Nucl Med Mol Imaging*. 2009;36:1434–1442.
20. Michel V, Yuan Z, Ramsuvar S, Bakovic M. Choline transport for phospholipid synthesis. *Exp Biol Med (Maywood)*. 2006;231:490–504.
21. Eiber M, Maurer T, Souvatzoglou M, et al. Evaluation of hybrid ^{68}Ga -PSMA ligand PET/CT in 248 patients with biochemical recurrence after radical prostatectomy. *J Nucl Med*. 2015;56:668–674.
22. Challapalli A, Trousil S, Hazell S, et al. Exploiting altered patterns of choline kinase-alpha expression on human prostate tissue to prognosticate prostate cancer. *J Clin Pathol*. 2015;68:703–709.
23. Schwarzenböck S, Souvatzoglou M, Krause BJ. Choline PET and PET/CT in primary diagnosis and staging of prostate cancer. *Theranostics*. 2012;2:318–330.
24. Maurer T, Gschwend JE, Rauscher I, et al. Diagnostic efficacy of ^{68}Ga -PSMA positron emission tomography compared to conventional imaging for lymph node staging of 130 consecutive patients with intermediate to high risk prostate cancer. *J Urol*. 2016;195:1436–1443.
25. Rauscher I, Maurer T, Fendler WP, Sommer WH, Schwaiger M, Eiber M. ^{68}Ga -PSMA ligand PET/CT in patients with prostate cancer: how we review and report. *Cancer Imaging*. 2016;16:14.